Steric Interactions Stabilize the Signaling State of the LOV2 Domain of Phototropin 1†

John M. Christie,*,‡,§ Stephanie B. Corchnoy,‡,|| Trevor E. Swartz,|| Mark Hokenson,|| In-Seob Han,⊥ Winslow R. Briggs,# and Roberto A. Bogomolni*,||

Plant Science Group, Division of Biochemistry and Molecular Biology, Institute of Biomedical and Life Sciences, University of Glasgow, University Avenue, Glasgow, Scotland, U.K., Department of Chemistry and Biochemistry, University of California, Santa Cruz, Santa Cruz, California 95064, Department of Biological Sciences, University of Ulsan, Ulsan, Korea, and Department of Plant Biology, Carnegie Institution of Washington, Stanford, California 94305

Received May 5, 2007

ABSTRACT: Phototropins (phot1 and phot2) are blue light receptor kinases that control a range of photoresponses that serve to optimize the photosynthetic efficiency of plants. Light sensing by the phototropins is mediated by a repeated motif at the N-terminal region of the protein known as the LOV domain. Bacterially expressed LOV domains bind flavin mononucleotide noncovalently and are photochemically active in solution. Irradiation of the LOV domain results in the formation of a flavin-cysteinyl adduct (LOV_{390}) which thermally relaxes back to the ground state in the dark, effectively completing a photocycle that serves as a molecular switch to control receptor kinase activity. We have employed a random mutagenesis approach to identify further amino acid residues involved in LOV-domain photochemistry. *Escherichia coli* colonies expressing a mutagenized population of LOV2 derived from *Avena sativa* (oat) phot1 were screened for variants that showed altered photochemical reactivity in response to blue light excitation. One variant showed slower rates of LOV_{390} formation but exhibited adduct decay times 1 order of magnitude faster than wild type. A single Ile → Val substitution was responsible for the effects observed, which removes a single methyl group found in van der Waals contact with the cysteine sulfur involved in adduct formation. A kinetic acceleration trend was observed for adduct decay by decreasing the size of the isoleucine side chain. Our findings therefore indicate that the steric nature of this amino acid side chain contributes to stabilization of the C−S cysteinyl adduct.

Plants possess a sophisticated array of photoreceptor pigments to detect and respond to changes in their surrounding light environment. In particular, UV-A/blue light (320−500 nm) acts as a stimulus to control many aspects of plant growth and development. Three distinct classes of plant photoreceptors mediate the effects of UV-A/blue light: cryptochromes, phototropins, and a new class of blue light receptors known as the ZTL/ADO family (*1*).

Cryptochromes (cry) play a major role in promoting plant photomorphogenesis (*2*) whereas the phototropins (phot) act to regulate light-dependent processes that serve to optimize the photosynthetic efficiency of plants and promote growth (*3*). Phototropins were first identified as photoreceptors for phototropism in *Arabidopsis thaliana* (*4*, *5*), but subsequent genetic analysis has shown that they function to regulate additional photoresponses including chloroplast relocation movements (*6*), light-induced stomatal opening (*7*), cotyledon and leaf expansion (*8*−*10*), and hypocotyl growth inhibition upon transfer of dark-grown seedlings to light (*11*). *Arabidopsis* contains two phototropins, phot1[1] and phot2, that share partially overlapping functions but exhibit different light sensitivities (*3*).

Primary amino acid structures of plant phototropins can be separated into two segments: a photosensory domain at the N-terminus and a serine/threonine kinase domain at the C-terminus. The N-terminal photosensory region of the phototropins contains two very similar domains of ∼110 amino acids designated LOV1 and LOV2. LOV (light, oxygen, and voltage) domains are members of the large and diverse superfamily of PAS (Per, Arnt, Sim) domains associated with cofactor binding and mediating protein−protein interactions (*12*). Both LOV1 and LOV2 function as blue light sensors (*13*) but exhibit different photochemical properties (*13*, *14*). Similarly, LOV1 and LOV2 have distinct functional roles in regulating photoreceptor activation (*14*−*16*). LOV2 plays an important role in regulating phototropin kinase activity and light-dependent receptor autophospho-

† Work in the authors' laboratories was supported by National Science Foundation Grants MCB 0091384 and MCB 0444504 to W.R.B. and MCB 0444390 and DMB-0090817 to R.A.B. and the award of a Royal Society University Research Fellowship to J.M.C. I.-S.H. was partially supported by a grant from the University of Ulsan.

* Corresponding authors. J.M.C.: e-mail, J.Christie@bio.gla.ac.uk; fax, +44 141 330 4447. R.A.B.: e-mail, bogo@chemistry@ucsc.edu; fax, (831) 459-2935.

‡ These authors contributed equally to the work.

§ University of Glasgow.

|| University of California, Santa Cruz.

⊥ University of Ulsan.

Carnegie Institution of Washington.

[1] Abbreviations: phot, phototropin; LOV, light, oxygen, or voltage; PAS, Per, Arnt, Sim; FMN, flavin mononucleotide; CD, circular dichroism; NMR, nuclear magnetic resonance.

10.1021/bi700852w CCC: $37.00
Published on Web 07/21/2007

rylation (*15*, *17*), while LOV1 has been proposed to mediate receptor dimerization (*18*, *19*) and/or modulate the photoreactivity of LOV2 (*20*, *21*).

Purification of milligram quantities of bacterially expressed LOV domains has greatly facilitated their spectral and structural characterization. Bacterially expressed LOV domains bind the blue light-absorbing cofactor flavin mononulceotide (FMN), enabling them to function as light sensors (*22*). Upon illumination, LOV domains undergo a photocycle that can be monitored by absorbance or fluorescence spectroscopy (*13*, *14*, *22*, *23*). In darkness, LOV domains bind FMN noncovalently, forming a fluorescent spectral species, designated LOV_{447}, which absorbs maximally near 447 nm (*13*, *22*, *23*). Irradiation of the domain induces the formation of a nonfluorescent covalent adduct between the C(4a) carbon of the flavin chromophore and a conserved cysteine residue within the LOV domain. Mutation of the cysteine to either alanine or serine results in a loss of photochemical reactivity (*13*).

Light-driven FMN-cysteinyl adduct formation occurs in the order of microseconds, producing a spectral species (LOV_{390}) that absorbs maximally at 390 nm (*13*, *14*, *23*). For phototropin LOV domains, formation of LOV_{390} is fully reversible in darkness, returning the LOV domain back to its initial ground state (LOV_{447}) within the order of ten to hundreds of seconds (*13*, *14*). Initial absorption of blue light by the FMN chromophore results in the formation of an excited singlet state, which decays into a flavin triplet state species (LOV_{660}) absorbing maximally in the red region of the spectrum (*23*−*25*). Although there is still some debate as to the reaction mechanism for LOV_{390} formation from the FMN triplet state (*26*, *27*), it is generally accepted that LOV_{390} represents the active signaling state that leads to photoreceptor activation.

To date, amino acid residues required for LOV-domain photochemistry and FMN binding have been identified through the availability of LOV1 and LOV2 crystal structures (*28*−*30*) in combination with site-directed mutagenesis (*13*). In the present study, we have developed an expression system in isolated *Escherichia coli* colonies to screen for novel LOV2 variants that exhibit impaired photochemical reactivity. In doing so, we have identified several mutants of LOV2 that exhibit altered photochemistry. The photochemical properties of these variants and related mutants produced by site-directed mutagenesis have been explored in detail. Our findings identify a highly conserved isoleucine residue within the LOV2 domain that plays an important role in the stabilization of LOV_{390} that is formed upon photoexcitation.

MATERIALS AND METHODS

PCR-Based Random Mutagenesis and Mutant Screening. An error-prone PCR library of the LOV2 domain of *Avena sativa* (oat) phot1 including the Jα-helix region (amino acids 404−559) was generated from the cDNA template using the Diversify PCR random mutagenesis kit (Clontech). The following sense and anitsense primers were used so that a 5′ *Eco*RI site and 3′ *Nco*I site were included in the PCR product to facilitate subsequent cloning: 5′-CGGAATTCT-TGGCTACTACACTTGAACG-3′ and 5′-GCGCCATGGT-TAGCCCACAAATCCTCT-3′. Final concentrations of 640 μM $MnSO_4$ and 80 μM dGTP were chosen for the PCR reaction to incorporate a mutagenesis frequency of 4.8 mutations/kb in accordance to the instructions of the supplier. The resulting PCR products were purified using QiaQuick PCR columns (Qiagen). After restriction enzyme digestion, purified PCR fragments were cloned into the pCALn-EK vector via *Eco*RI and *Nco*I. Ligation reactions were transformed into electrocompetent BL21(DE3) *E. coli* (Novagen), plated on LB agar containing 100 μg/mL ampicillin (Sigma) and 100 μM IPTG (Roche), and incubated in complete darkness at 30 °C for 24 h. LOV-domain fluorescence and activity in isolated *E. coli* colonies were monitored using a Lecia MZ-12 dissecting fluorescence microscope.

Site-Directed Mutagenesis. Single amino acid mutations were introduced by using the QuikChange site-directed mutagenesis kit (Stratagene) in accordance with the instructions of the supplier. All amino acid changes were verified by DNA sequencing.

Protein Sample Preparation. Protein samples (the LOV2 domain of oat phot1 and respective mutants) were prepared as described previously (*13*, *22*). LOV domains were expressed in *E. coli* and purified by calmodulin affinity chromatography (Stratagene). Purified samples were dialyzed against Tris buffer (20 mM Tris, 50 mM NaCl, pH 8) using Slide-A-Lyzer cassettes (Pierce) and concentrated using centrifugal concentrators (Continental Lab Products). Protein samples were centrifuged and/or filtered through a 0.2 μm filter prior to use. Protein concentrations were determined by absorption spectroscopy using a Hewlett-Packard 8452 diode array spectrophotometer. The concentration was determined using $\epsilon_{447}(\mathrm{LOV2}) = 13800\ \mathrm{M^{-1}\ cm^{-1}}$ (*13*).

Light-Induced Absorption Changes at Short Times. Absorbance difference spectra in the 30 ns to 690 ms time window were collected using an instrument described previously (*31*). A dye laser pumped by the third harmonic of a Nd:YAG laser provided a 10 ns, 80 $\mu J/mm^2$ light pulse at 477 nm. A fresh sample was provided for each laser flash, allowing the averaging of absorbance data of several samples. The laser pulse traversed the sample perpendicular to the path of white light from a flashlamp that was used to probe the absorbance change in the sample. The optical path lengths for the probe light and laser were 2 and 0.5 mm, respectively. The white light used to probe absorbance was linearly polarized at the magic angle (54.7°) relative to the laser polarization axis to prevent rotational diffusion (*32*). The temperature for all measurements was 20 °C.

Light-Induced Changes at Long Times. Absorbance difference spectra in the 1−100 s time range were collected using a Shimadzu MultiSpec-1501 diode array spectrophotometer at room temperature. The optical path length was 0.5 cm, and a white light camera strobe flash provided the excitation pulse. All protein samples were analyzed under these conditions.

Global Analysis. Data were analyzed using programs written in a Matlab environment (The Mathworks) as described previously (*23*). Briefly, data matrices were constructed and subjected to singular value decomposition followed by global exponential fitting. Kinetic changes at all measured wavelengths were decomposed into a sum of exponential components. The exponents contained the apparent rate constants for the observed kinetic changes, and the amplitudes at different wavelengths represented the

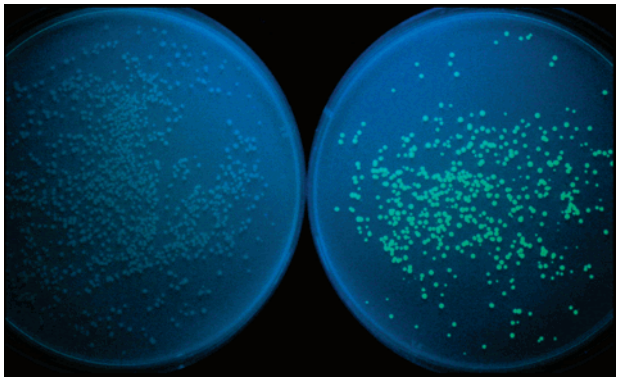

FIGURE 1: LOV2 fluorescence in isolated *E. coli* colonies grown on agar medium. *E. coli* were transformed with empty expression vector (left) or with vector carrying the cDNA sequence encoding the LOV2 domain of oat phot1 (right). *E. coli* expressing LOV2 emit strong green fluorescence compared to the vector only control when viewed under UV light.

spectral changes associated with the exponential process and were designated b-spectra.

D_2O Exchange. Protein samples were divided into two equivalent aliquots and were lyophilized overnight in the dark as described previously (*23*). One aliquot was then reconstituted in H_2O and the other in D_2O.

Circular Dichroism Spectroscopy. Purified protein samples were dialyzed against Tris buffer (5 mM Tris, 5 mM NaCl, pH 8). CD spectra were recorded using an Aviv 60DS CD spectrometer as described previously (*33*). Spectra were collected at 20 °C. In the visible/near-UV region (260−500 nm) 15 μM protein was used in a 1 cm path length rectangular cuvette; in the far-UV region (190−250 nm) 7 μM protein was used in a 0.1 cm path length rectangular cuvette.

RESULTS

Isolation of LOV2 Variants. E. coli colonies grown on standard agar medium, expressing the LOV2 domain of *A. sativa* (oat) phot1 emit a strong green fluorescence upon excitation with UV/blue light (Figure 1) owing to the inherently bound FMN chromophore. Colonies become nonfluorescent when irradiated with saturating blue light as a result of flavin-cysteinyl adduct formation within the chromopeptide. The fluorescence state of LOV2 expressed in *E. coli* colonies can be monitored readily using a dissecting fluorescence microscope. Furthermore, the effect is fully reversible upon transfer of colonies to darkness for 1−2 min (data not shown). The time scale of fluorescence recovery observed for LOV2-expressing *E. coli* coincides with the rate of adduct decay reported for purified oat phot1 LOV2 in solution (*13*, *14*, *23*). Hence, LOV-domain expression in *E. coli* colonies provides a convenient and rapid means to screen populations of mutated LOV domains and identify novel variants with altered photochemical properties.

We used PCR-based random mutagenesis to generate a library of mutagenized LOV2-encoding DNA sequences that were cloned into the bacterial expression vector pCALn-EK, routinely used for LOV-domain expression in *E. coli* (*13*, *14*, *22*, *23*). As a result, LOV domains were expressed as calmodulin binding peptide (CBP N-terminal) fusions to facilitate subsequent protein purification via calmodulin affinity chromatography. The mutagenized population of LOV2 was transformed into *E. coli* and plated on standard agar medium. Over 16000 colonies were screened under a dissecting fluorescence microscope for mutants that did not exhibit any detectable fluorescence loss upon blue light excitation. A total of 60 such colonies were obtained, plasmid DNA was isolated, and the corresponding lesions within the LOV2 domain were determined by DNA sequencing. In many cases, more than one point mutation was detected which corresponded to the mutation frequency employed in the random mutagenesis procedure (see Materials and Methods). However, a large number of mutations were found to be silent, causing no change in the amino acid sequence. Indeed, a small percentage of LOV2 variants rescued (10%) exhibited no detectable change in protein sequence and were discounted as false positives. Despite this result, several amino acid residues were identified as common targets for mutagenesis (Table 1).

Table 1: Random Mutagenesis of LOV2[a]

amino acid change	mutation	% frequency
I16V	AAT → GTT	15
I16T	AAT → ACT	2
K2R/I16V	AAG → AGG/AAT → GTT	32
C39S	TGC → AGC	20
C39G	TGC → GC	15
N38G	AAC → GAC	2
N38S	AAC → AAG	2
Q43H	CAA → CAT	2

[a] Mutations identified from the *E. coli* mutant screen that result in a lack of fluorescence loss upon blue light excitation. The frequency of occurrence of each mutation is indicated.

One-third of the mutations recovered were found to alter the conserved active site cysteine residue that forms a covalent adduct with the C(4a) carbon of the FMN chromophore upon photoexcitation. For simplicity, we refer to this cysteine as Cys^{39} as introduced by Salomon et al. (*13*), based on the relative position of this amino acid residue within the isolated LOV2 domain (Cys^{450} in full-length oat phot1). A small percentage of mutations were found to alter amino acid residues in close proximity to Cys^{39}, namely, Asn^{38} and Gln^{43} (Table 1). These findings are consistent with earlier site-directed mutagenesis studies reporting that mutations in either Asn^{38} and Glu^{43} reduce the photochemical reactivity of oat phot1 LOV2 (*13*). The majority of mutations detected (~50%) were located within a conserved isoleucine residue, Ile^{16}. The most frequent mutation found associated with Ile^{16} was subtle, in that the isoleucine residue was conservatively replaced by valine (Table 1). Variants harboring this amino acid change were chosen for further analysis as mutations within Ile^{16} had not been reported previously.

Spectroscopic Analysis of the K2R/I16V Double Mutant. The majority of the I16V variants identified contained a second amino acid substitution in which a conserved lysine at amino acid position 2 within LOV2 was replaced by arginine (Table 1). Given its prevalence, this mutant was selected for detailed photochemical characterization. As shown in Figure 2, the UV−visible absorption spectrum of the K2R/I16V double mutant is almost identical to that of wild type. LOV2 shows a single absorption maximum at about 375 nm with a slight shoulder at shorter wavelengths. This shoulder appears to be more pronounced for the K2R/I16V double mutant and may reflect subtle changes in the

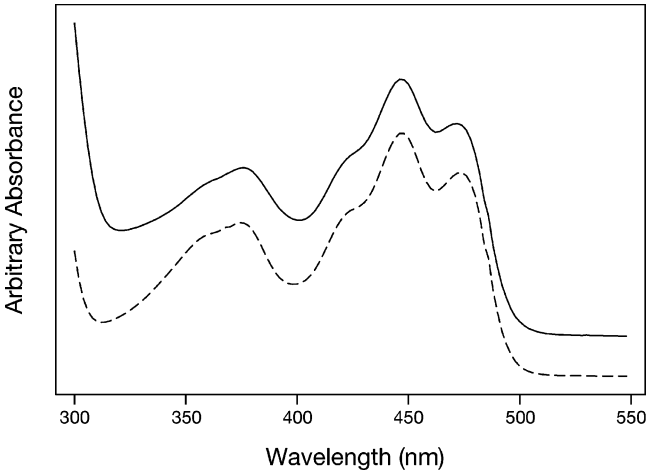

FIGURE 2: Absorption spectra of wild-type LOV2 (solid line) and the K2R/I16V double mutant (dashed line). Spectra are offset for clarity.

electrostatic environment of the chromophore. However, given the high degree of similarity in absorbance properties between the wild type and mutant chromopeptides, we conclude that no major structural or electrostatic changes occur within the vicinity of the FMN chromophore as a result of the mutations introduced.

Possible structural changes resulting from the K2R and I16V substitutions were probed in greater detail by circular dichroism (CD) spectroscopy. CD spectra of LOV domains in the visible/near-UV reflect primarily the contributions from the bound FMN chromophore and the environment of aromatic side chains (*33*). To allow for direct comparison, CD spectra were offset to a region of zero CD signal (500 nm). Wild-type LOV2 exhibited negative bands near 270, 380, 450, and 475 nm and a weak positive band in the 310−350 nm region of the spectrum (Figure 3A). The intensity of the positive band was higher for the K2R/I16V double mutant, possibly indicative of subtle structural changes within the chromophore environment. Yet, the close similarity between the visible/near-UV CD spectra again suggests that no major structural changes were introduced into the chromophore-binding environment by the two mutations.

CD spectra of LOV domains in the far-UV reflect primarily protein secondary structure as the FMN chromophore exhibits comparatively little CD activity in this spectral region (*33*). As above, far-UV CD spectra were offset to a region of zero CD signal (250 nm) to allow for direct comparison. Spectra obtained for the wild-type and mutant proteins showed two negative bands at approximately 222 and 208 nm and a positive band at around 195 nm (Figure 3B). Such properties are routinely observed for proteins containing significant amounts of α-helix and *β*-sheet conformations (*34*). The negative bands at 208 and 222 nm are slightly less intense for the mutant protein relative to that of wild-type LOV2. This difference may correspond to minor changes in the arrangement of secondary structural features due to the replacement of Ile^{16} with the more compact valine inside the LOV2-core, as well as substitution of Lys^{2} with the more bulky arginine. However, the overall similarity observed between these spectra is consistent with the small differences detected in the visible/near-UV region (Figure 3A) and by UV−visible absorption spectroscopy (Figure 2), indicating that any changes in protein secondary

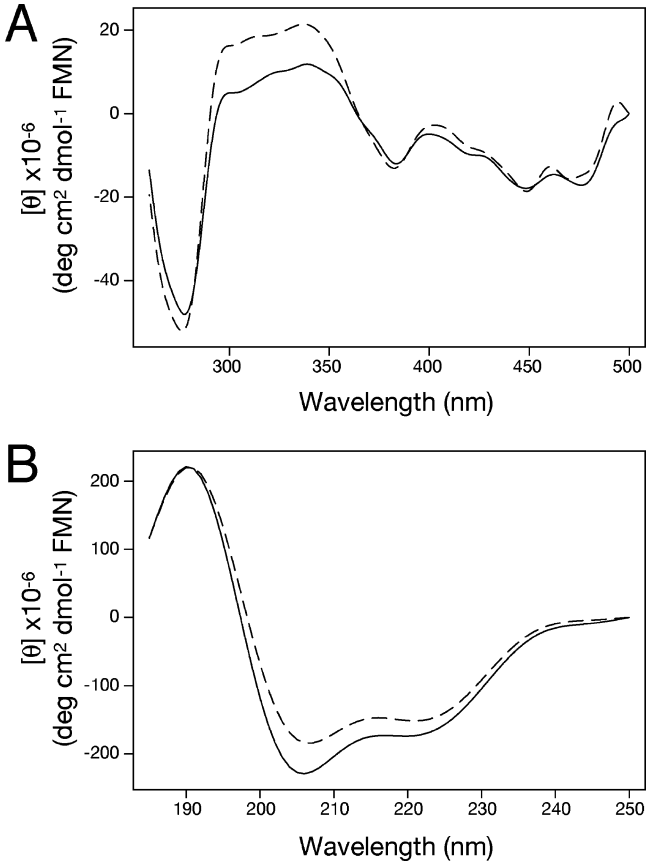

FIGURE 3: CD spectra of wild-type LOV2 (solid line) and the K2R/I16V double mutant (dashed line) in the visible/near-UV (A) and far-UV (B) regions.

structure arising from the two point mutations are likely to be minimal.

Light-Driven Adduct Formation in the K2R/I16V Double Mutant Is 2-fold Slower Than in Wild Type. Nanosecond laser flash spectroscopy has shown that irradiation of LOV2 results in the formation of a transient ~660 nm absorbing flavin triplet state intermediate (LOV_{660}) that subsequently decays into a 390 nm absorbing metastable flavin-cysteinyl adduct (LOV_{390}) with a time constant of 6 *μ*s (*23*, *33*). We used the same approach to determine the rate of adduct formation from the triplet state for the K2R/I16V double mutant. The difference absorption spectrum corresponding to the earliest time measurement after the excitation flash (30 ns) showed bleaching of the visible flavin absorption band at 447 nm and the appearance of LOV_{660} with long-wavelength absorption near 660 nm (Figure 4, upper panel). These spectral properties are consistent with those observed previously for the LOV2 domain of oat phot1 (*23*). Global kinetic analysis resulted in a single exponential decay of LOV_{660} with a time constant of 6 *μ*s. Kinetic analysis produced two b-spectra (Figure 4, lower panel) that represent spectral changes associated with the exponential decay process. As reported for the LOV2 domain of oat phot1 (*23*), approximately half the amount of absorbance bleaching occurring at 450 nm in the 30 ns difference spectrum remained in the 1 ms spectrum, suggesting that 50% of the triplet state decays to form LOV_{390} whereas the other 50% returns to the initial ground state form. Hence, the calculated time constant for adduct formation for the K2R/I16V double mutant is 12 *μ*s, 2-fold slower than that detected previously for LOV2 of oat phot1 (*33*).

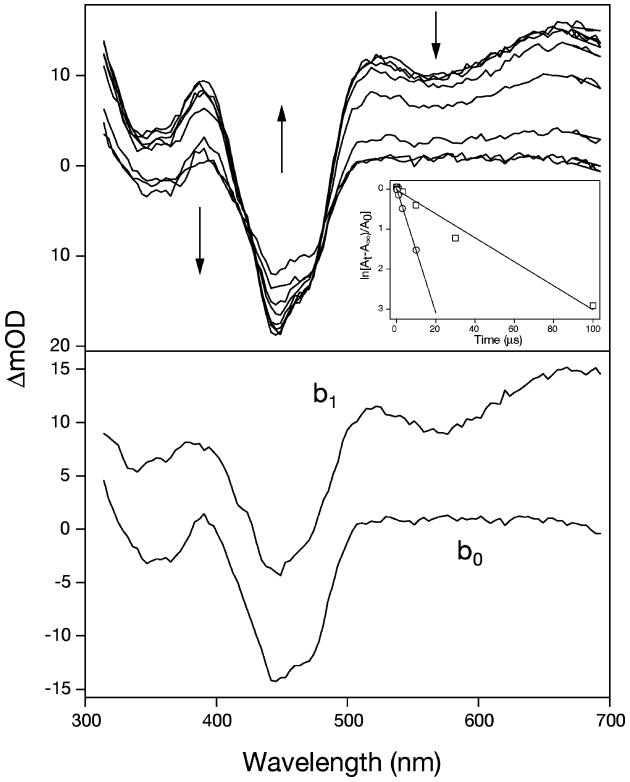

FIGURE 4: Nanosecond laser flash spectroscopy of the K2R/116V double mutant. Difference spectra recorded in H_2O at 0.03, 0.13, 0.33, 1, 3, 10, and 100 μs and 690 ms (upper panel). Arrows indicate the direction of change over time. Results of global exponential fitting of the difference spectra are shown in the lower panel. The b-spectrum b_1 has an apparent time constant of 6 μs, and b_0 is the difference spectrum of the product formed. The inset illustrates the 4-fold slowing of the triplet decay in D_2O (□) relative to H_2O (○).

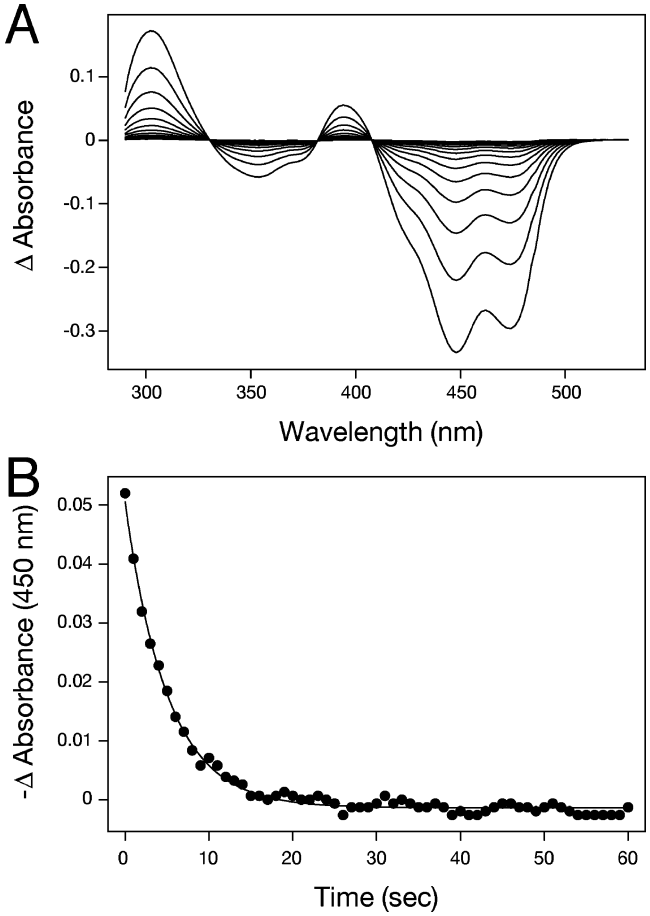

FIGURE 5: Time-resolved light-induced absorption changes for the K2R/I16V double mutant. (A) Absorption difference spectra showing the return of the mutant to the dark form following photoexcitation. Spectra were recorded every 2 s. (B) Absorption changes after light excitation measured at 450 nm for the K2R/I16V double mutant. Decay fits to a single exponential (solid line) with a time constant of 5 s.

The rate of adduct formation for the K2R/I16V double mutant was also measured in the presence of D_2O. Solvent kinetic isotope effects reported for light-driven adduct formation in the LOV2 domain of oat phot1 indicate that the rate-limiting step of the reaction requires proton transfer(s) involving exchangeable protons (*33*). Global kinetic analysis of the measured difference spectra obtained for the K2R/I16V double mutant reconstituted in D_2O showed a single exponential decay of the flavin triplet state with a time constant of 25 μs (Figure 4, inset). Taking the back-reaction into account, the calculated time constant is 50 μs, approximately 4-fold slower than that observed in H_2O. The calculated b-spectra were consistent with the b-spectra obtained for the K2R/I16V double mutant in H_2O (data not shown). Moreover, the observed 4-fold decrease in rate of adduct formation for the K2R/I16V double mutant in D_2O is comparable to that observed for wild-type LOV2 (*33*), suggesting that the rate-limiting proton transfer(s) involved in LOV_{390} formation is (are) unaffected in D_2O by the K2R and I16V point mutations.

Adduct Decay for the K2R/I16V Double Mutant Is 10-fold Faster Than for Wild Type. Absorption difference and fluorescence spectroscopies have shown that the LOV2 domain of plant phototropins relaxes from the flavin-cysteinyl adduct form to the dark state with a time constant of about 60 s (*13*, *14*, *23*). We therefore measured the rate of adduct decay for the K2R/I16V double mutant by absorbance difference spectroscopy. The light-minus-dark absorption difference spectra obtained (Figure 5A) were consistent with those for the LOV2 domain of oat phot1 (*23*). Irradiation of the double mutant results in a rapid loss of absorption in the blue region of the spectrum and a concomitant shift of the near-UV absorption band at 370 nm to one at 390 nm. The LOV_{390} photoproduct and the initial ground state (LOV_{447}) of the K2R/I16V double mutant share three isosbestic points, at approximately 331, 385, and 407 nm. These properties are almost identical to those for wild-type LOV2 and correspond to the formation of the FMN-cysteinyl adduct within the domain (*13*, *23*).

The kinetics of adduct decay for the double mutant, analyzed via singular value decomposition and exponential fitting, indicate a single exponential decay to the dark form with no other spectrally observed intermediates (Figure 5B). Remarkably, kinetic analysis derived a time constant for adduct decay of 5 s for the K2R/I16V double mutant, 1 order of magnitude faster than that reported for the LOV2 domain of oat phot1 (*13*, *23*). Hence, the faster dark-recovery kinetics of the double mutant compared to its wild-type counterpart most likely accounts for its fluorescence phenotype detected under the light conditions of our mutant screen. The steady-state concentration of LOV2 molecules in the adduct form would decrease under moderate light intensities, owing to a faster back-reaction, and result in a more fluorescent phenotype.

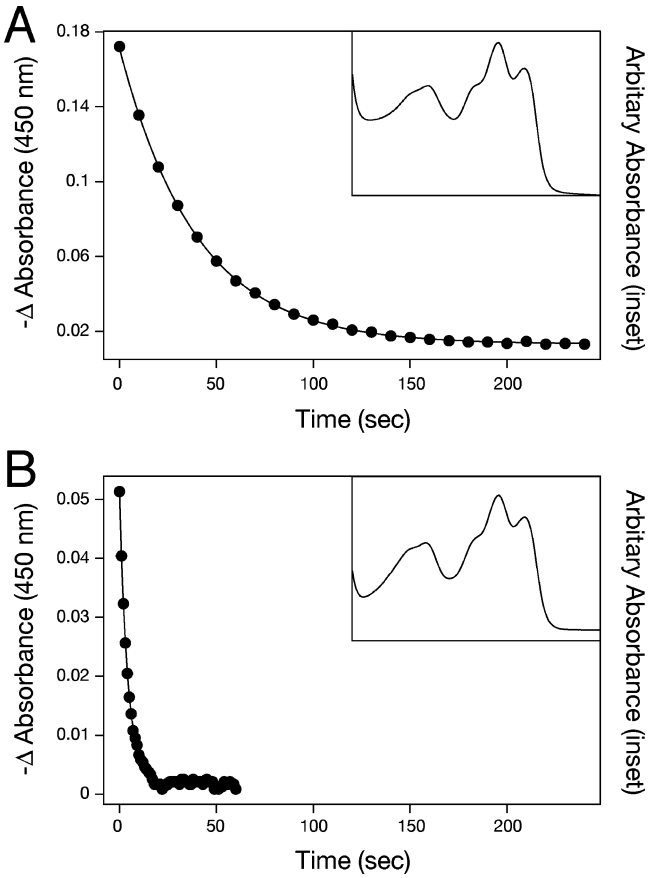

FIGURE 6: Time-resolved light-induced absorption changes for the single K2R and I16V mutants. Absorption changes after light excitation measured at 450 nm for the K2R mutant (A) and the I16V mutant (B). Decays fit to a single exponential (solid lines) and indicate a time constant of 40 and 4 s for the K2R mutant and I16V mutant, respectively. Absorption spectra of the respective mutants are also shown (insets).

The I16V Mutation Mediates Rapid Recovery. Given the above findings, it was important to establish whether the K2R or the I16V mutation was responsible for the fast recovery kinetics observed. The respective single mutants were generated and their dark recovery kinetics probed using absorbance difference spectroscopy. The absorption spectra for the K2R and I16V single mutants were almost identical to that of wild-type LOV2 (Figure 6, inset). Incorporation of the single K2R mutation within the LOV2 domain of oat phot1 did not appear to alter the kinetics for adduct decay relative to that of the wild-type protein (Figure 6A). Kinetic analysis derived a time constant for adduct decay of 40 s for the K2R single mutant compared to 37 s obtained for wild-type LOV2 (data not shown), which agrees well with previously reported values for phot1 LOV2 domains (*13*, *14*, *23*). Similarly, the rate of adduct formation measured for the K2R single mutant was found to be 5 μs (data not shown), corresponding to that measured for wild-type LOV2 (*23*, *33*). Together, these findings indicate that the effects observed on both the rates of adduct formation and adduct decay for the K2R/I16V double mutant result primarily from the I16V mutation. In agreement with this conclusion, LOV2 harboring the single I16V mutation was found to exhibit rapid dark recovery kinetics (Figure 6B). The time constant for adduct decay calculated for the I16V single mutant was 4 s, which coincided closely to that obtained for the K2R/I16V double mutant, indicating that the fast rate of recovery can be attributed to the I16V mutation. Therefore, these fast recovery properties account for the fluorescence phenotype observed for the single I16V variant identified from the *E. coli* colony screen (Table 1). Such fast recovery properties are also likely accountable for the fluorescent phenotype detected for mutations in Asn[38] (Table 1), as replacement of Asn[38] with serine was found to increase the rate of adduct decay dramatically for LOV2 with an estimated time constant of <1 s (Supporting Information, Figure 1).

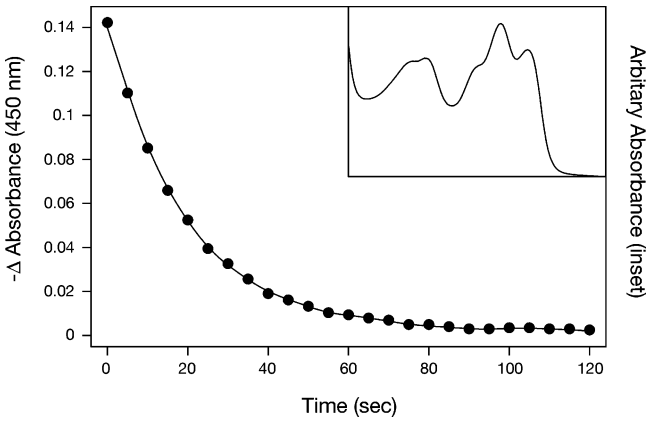

FIGURE 7: Time-resolved light-induced absorption changes for the K2R/I16L double mutant. Absorption changes after light excitation measured at 450 nm. Decay fits to a single exponential (solid lines) and indicates a time constant of 19 s. Absorption spectrum of the K2R/I16L double mutant is also shown (inset).

Table 2: Effect of Side Chain Replacement of Ile[16] on the Rate of Adduct Decay of LOV2[a]

		adduct decay (s)		
amino acid (position 16)	residue mass (Da)	Tris buffer	H_2O	D_2O
isoleucine	113.2	40	35	111
leucine	113.2	19	19	77
valine	99.1	5	5	23

[a] Time constants for adduct decay are indicated for two independent substitutions of Ile[16] in Tris buffer (20 mM Tris, 150 mM NaCl, pH 8.0) or reconstituted in H_2O or D_2O. All variants, including Ile[16], contained the second K2R mutation.

Further Side Chain Change Replacement of Ile[16]. Ile → Val is a conservative amino acid substitution that results in the loss of a methyl group. It was therefore of particular interest that such a small change would result in adduct decay kinetics 1 order of magnitude faster than wild type. To investigate the role of Ile[16] on adduct decay in more detail, we created a K2R/I16L double mutant. The absorption spectra obtained for this mutant were very similar to that of wild-type LOV2 (Figure 7, inset), indicating that the I16L mutation brought about no major structural or electrostatic changes. Adduct decay kinetics for the K2R/I16L double mutant were faster than those detected for wild-type LOV2 (Figure 7) with a time constant of 19 s (Table 2). As summarized in Table 2, altering the size of the side chain at amino acid position 16 results in faster time constants for adduct decay. The fastest rate of adduct decay was found for the K2R/I16V double mutant. Rapid kinetics for adduct decay were also detected for the I16T single mutant identified from the *E. coli* colony screen (Table 1), resulting in an estimated time constant of <2 s (Supporting Information, Figure 2). Together, these findings indicate that the side chain of Ile[16] contributes to stabilization of the FMN-cysteinyl

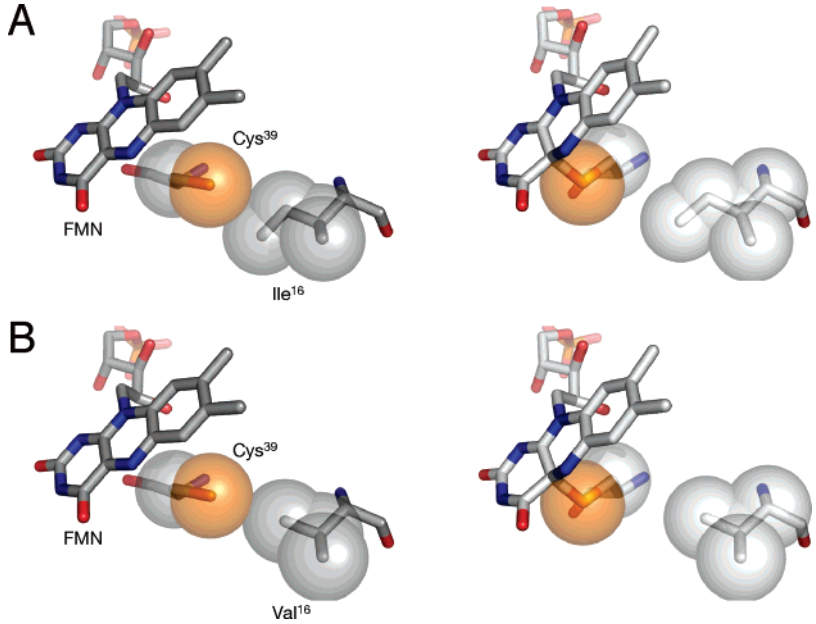

FIGURE 8: Localized structural impact of the I16V mutation within the FMN-binding pocket of LOV2. The LOV2 domain of oat phot1 was obtained by homology modeling with the program Swiss Model (http://www/expasy/org) using the dark and light protein structures of *Adiantum* neochrome LOV2 (PDB entries 1G28 and 1JNU, respectively). Images were created using PyMOL. (A) In the wild-type domain, Ile^{16} forms van der Waals contacts with residue Cys^{39} in the dark state (left). In the photoexcited state (right), the side chain of Ile^{16} moves to accommodate the space created upon FMN-cysteinyl adduct formation. (B) Replacement of Ile^{16} with valine diminishes van der Waals contacts with the Cys^{39} in the dark state (left). The valine side chain is also unable to fill the space created by movement of the Cys^{39} sulfur upon adduct formation in the photoexcited state (right) that is normally occupied by the δ-carbon atom of Ile^{16}.

adduct formed upon irradiation and that progressively decreasing the size of this side chain results in faster rates of adduct decay. We have also created a K2R/I16A double mutant of LOV2. Preliminary analysis indicates that this variant exhibits an absorption spectrum similar to that of the K2R/I16V double mutant but shows reduced photobleaching (data not shown) and requires additional analysis to assess the effect of the I16A mutation on the kinetics of adduct decay.

The rates of adduct decay for the K2R/I16L and K2R/I16V double mutants and the K2R single mutant were also measured in the presence of D_2O. Adduct decay for wild-type LOV2 is three times slower in D_2O than H_2O (*23*), indicating that proton transfers are involved in the rate-limiting steps during this process. In each case, the rate of adduct decay for samples reconstituted in H_2O coincided with the decay rates measured for the original samples (Table 2). Moreover, the kinetics of adduct decay observed for each reconstituted sample fit single exponential decays in both H_2O and D_2O (data not shown). A comparable 3−4-fold slowing effect of D_2O was detected for the rate of adduct decay for each of the protein samples analyzed (Table 2). These findings indicate that the native, rate-limiting proton transfers involved in the adduct decay process are unaffected by the introduced mutations.

DISCUSSION

E. coli Colony Expression Offers a High-Throughput Means To Isolate Novel LOV Variants. Directed evolution is a powerful technique used to study protein structure and function. This approach has been used successfully to engineer photoreceptor molecules to exhibit novel photochemical properties, including green fluorescent protein (GFP) from the jellyfish *Aequorea victoria* (*35*) and more recently a cyanobacterial phytochrome (*36*). A similar approach was employed in this study to isolate variants of the LOV2 photosensory region of the phot1 blue light receptor that exhibit altered photochemical properties. The role of the highly conserved residue Cys^{39} in the reaction mechanism for LOV-domain photochemistry was highlighted by our screening procedure as over a third of the mutants obtained showing altered fluorescence properties contained an alteration within the codon for this amino acid residue (Table 1). An equivalent cysteine residue is also necessary for the photochemical reactivity of a diverse range of LOV-sensor proteins found in plants, fungi, and a variety of prokaryotes (*37*, *38*). It should now be possible to use the approach described here for the directed evolution of other LOV-sensing motifs. Refinement of the screening procedure should also allow the isolation of mutants with desired photochemical traits.

Potential Structural Consequences of the I16V Mutation. In screening for fluorescence variants of LOV2, we uncovered a mutational hot spot, residue Ile^{16} (Table 1), that when mutated to valine fails to show detectable fluorescence loss in *E. coli* colonies under the light conditions used. While much of our work focused on the K2R/I16V double mutant, our findings from single mutant analyses indicated that the K2R mutation represents a second mutational hot spot that has little, if any, effect on LOV-domain photochemical reactivity (Figure 6). Indeed, the crystal structure of neochrome (formerly phy3) LOV2 from the fern *Adiantum capillus-veneris* indicates that Lys^2 is distantly located from the site of LOV-domain photochemistry, while Ile^{16} is located in close proximity and within van der Waals contacts to the sulfhydral group of Cys^{39} (*30*).

The known structure of neochrome LOV2 can be used to model the chromophore environment of the LOV2 domain

of oat phot1 (Figure 8A). On the basis of this model, mutation of Ile^{16} to valine in the LOV2 domain of oat phot1 reduces contacts with Cys^{39} via elimination of the side chain δ-carbon arising from the I16V mutation (Figure 8B). As a result, the protein would be energetically driven to compensate for the space generated via small structural adjustments, such as shifting of the Cys^{39} sulfur back toward the γ-carbon of the introduced valine and away from the chromophore, in an attempt to recover van der Waals contacts. From the homology model, the side chains in closest proximity to Ile^{16} (within 5 Å) correspond to Val^{5}, Phe^{23}, Ile^{34}, Cys^{39}, and Phe^{41}, indicating primarily a hydrophobic region. Removal of the δ-carbon methyl group of Ile^{16} would be expected to compromise this hydrophobic region by increasing the distances between side chain atoms. Consequently, shifts in the neighboring hydrophobic residues could occur to help maintain the structural integrity and/or solvent exclusion roles that this region may contribute in the native protein. Taken together, the possible structural compensations associated with Cys^{39} and the surrounding hydrophobic residues would be expected to manifest as slight spectral changes that may correspond to those detected by near- and far-UV CD spectroscopy (Figure 3). These spectral properties as well as the native-like absorption spectra (Figures 2, 6, and 7) provide strong support that the proteins analyzed throughout this study harboring both double and single point mutations undergo only slight structural changes relative to wild type in the dark state.

We also sought to probe spectrally structural perturbations that may occur in response to LOV_{390} formation in the K2R/I16V double mutant. The light-minus-dark far-UV CD difference spectrum for the LOV2 domain of oat phot1 resembles the spectrum of an inverted α-helix, suggesting that α-helicity is lost upon irradiation (*33*). These findings are consistent with recent solution NMR spectroscopy analysis showing that photoexcitation of LOV2 leads to the displacement of a conserved amphipathic α-helix, Jα, from the surface of the LOV2 core (*39*) that is required to bring about activation of the C-terminal kinase domain and in turn receptor autophosphorylation (*17*, *40*). This light-induced structural change has recently been confirmed by far-UV time-resolved optical rotatory dispersion spectroscopy (*41*) and pulse laser induced transient grating (*42*). Unfortunately, the light-induced far-UV CD spectrum could not be measured for the K2R/I16V double mutant owing to the accelerated back-reaction of this variant. Even at 2 °C, the rate of adduct decay for the double mutant was too fast to collect CD spectra under our experimental conditions (data not shown).

Loss of Steric Interaction between Ile^{16} and Cys^{39} Slows Adduct Formation. Our findings suggest that the I16V mutation causes two unique impacts. It decreases the rate of adduct formation 2-fold and increases the rate of adduct decay by almost a factor of 10. We propose that both effects are caused by the loss of steric support near the active site cysteine residue owing to the I16V mutation. Furthermore, the steric support provided by Ile^{16} differs between dark and photoexcited states of the protein (Figure 8A).

As described above for the I16V mutation, removal of the δ-carbon of Ile^{16} disrupts native van der Waals contacts (Figure 8B) and may result in slight movement of the sulfur atom of Cys^{39} back toward the valine γ-carbon atom and away from the FMN chromophore. Consequently, it would be energetically less favorable for the sulfur atom to move toward the FMN to promote C−S bond formation. The dark state crystal structure of *Adiantum* neochrome LOV2 shows that the sulfur of Cys^{39} is situated 4.2 Å from the C(4a) carbon of the FMN chromophore (*30*). By contrast, the photoexcited structure of neochrome LOV2 shows that the sulfur of Cys^{39} moves to within 1.8 Å of the chromophore (*29*). The δ-carbon of Ile^{16} may therefore serve to limit the conformational space available to the sulfur atom in the dark state, thereby facilitating formation of the C−S bond upon photoexcitation. In the absence of the isoleucine δ-carbon atom, the sulfur atom may occupy a larger conformational space reducing the native predisposition toward C−S bond formation. Such an effect would manifest as a decrease in the rate of adduct formation, consistent with the relatively modest 2-fold decrease measured for the K2R/I16V double mutant (Figure 4).

Conformational Strain May Drive Adduct Decay. A mechanistic model involving structure-stabilizing interactions between the sulfur of Cys^{39} and the side chain of Ile^{16} implies that, as adduct formation was slowed by the I16V mutation, adduct decay should be faster in the mutant. That is, light-induced displacement of the sulfur atom toward the C(4a) carbon of the FMN chromophore would be less favorable in the presence of the I16V substitution whereas the energetic drive to return to its original position would be stronger. Indeed, the kinetics of adduct decay were increased dramatically (about 1 order of magnitude) by the I16V mutation (Table 2). The large magnitude of the effect observed suggests that the native isoleucine side chain plays a unique and direct role in stabilization of the adduct state of LOV2. In fact, the photoexcited structure of neochrome LOV2 shows that the side chain of Ile^{16} moves approximately 1 Å toward the space vacated by the active sulfur atom with the δ-carbon of Ile^{16} moving the furthest (*29*). By moving toward the sulfur atom in this way (Figure 8A), the isoleucine side chain may provide direct steric support for generation of the C−S bond, mirroring our proposed model for its role in the adduct formation process. Removal of the δ-carbon atom as in the I16V mutant would diminish such steric support (Figure 8B), potentially resulting in substantial conformational strain acting against the flavin-cysteinyl adduct.

Recent solution NMR measurements of the adduct state of wild-type LOV2 of oat phot1 reveal significant movement of residues near the chromophore, as well as broader tertiary structure changes separate from those associated with the signal transduction process involving the Jα-helix (*39*, *43*). We considered that some of these light-induced protein motions could contribute to moderation of the adduct decay rate in the native protein. The small structural perturbations we observed for the dark state of the I16V mutant, which may include disturbance of the hydrophobic region surrounding the δ-carbon of Ile^{16}, could subsequently hinder adduct-stabilizing motions that would normally occur within LOV2 and throughout the native protein upon irradiation. The combination of a discrete steric effect within the LOV2 core and a subsequent reverberation throughout the domain in the form of hindered protein motions upon irradiation would imply a critical role for the δ-carbon of Ile^{16} in the adduct decay mechanism. Such steric and structural effects that are primarily relevant to the photoexcited state of the protein (LOV_{390}) would be consistent with the small effect on

kinetics of adduct formation and the larger effect on the kinetics of adduct decay observed for the I16V mutant.

Further mutagenesis supports the conclusion that the side chain of Ile[16] plays a direct role in stabilization of the adduct state. Mutation of Ile[16] to leucine resulted in a modest 2-fold acceleration of the rate of adduct decay compared to wild type (Figure 7, Table 2). While valine has no side chain δ-carbon, leucine is an isomer of isoleucine with two δ-carbon atoms instead of one. The slight acceleration of adduct decay observed for the I16L mutant would be expected if the presence of the additional δ-carbon alters native, light-driven support of the C−S bond. The bulkier leucine side chain may be sterically hindered from moving as far toward the sulfur atom of Cys[39], providing weaker support for the C−S bond and potentially hindering other light-driven conformational changes that typically occur in the wild-type protein. Likewise, substitution of Ile[16] with threonine would also be expected to reduce side chain contacts with Cys[39] and also resulted in faster rates of adduct decay (Supporting Information, Figure 2), once again highlighting the steric importance of the Ile[16] δ-carbon.

It is unclear at present whether the equivalent residue in LOV1 serves a similar function. Collective alignment of LOV1 and LOV2 from plant phototropins shows that residue Ile[16] is highly conserved between the domains (*44*). One exception is the LOV1 domain from the phototropin from the green alga *Chlamydomonas rheinhardtii*, whereby the amino acid residue equivalent to Ile[16] is a leucine. Substitution of the aforementioned leucine with isoleucine has been reported to moderately increase the rate of adduct decay for the LOV1 domain of *Chlamydomonas* phot (*45*). This is in contrast to the results presented here suggesting that mutation of the residue at position 16 may result in different consequences in LOV1 relative to LOV2.

CONCLUSIONS

Taken together, our findings demonstrate that the conserved isoleucine side chain at amino acid position 16 within LOV2 plays a unique and specific role in the adduct decay mechanism and highlights the particular importance of the side chain δ-carbon. Imidazole has recently been reported to accelerate adduct decay of LOV2 by several orders of magnitude via a base-catalyzed mechanism (*46*). A similar effect of imidazole has been observed for the K2R/I16V double mutant isolated in the present study (M. T. A. Alexandre and J. T. M. Kennis, personal communication). Thus, the mode of action of imidazole appears to be independent of the steric role of Ile[16], indicating that several factors contribute to the mechanism of adduct decay. Our mutagenesis analysis provides evidence for additional residues that are important for this process. Mutations in Asn[38] also lead to an acceleration of adduct decay (Supporting Information, Figure 1). Similarly, mutations in Gln[43] have been reported to result in a reduction of LOV2 photochemical reactivity (*13*), making it tempting to speculate that mutations within this residue also give rise to fast recovery rates that account for the fluorescence phenotype observed for the Q43H variant isolated from our screen (Table 1). The side chain of Gln[43], like that of Asn[38], hydrogen bonds with the ribityl chain of the FMN chromophore (*30*). Moreover, the position of Gln[43] adjusts to the displacement of the FMN chromophore upon photoexcitation (*29*). Mutations in Gln[43] and Asn[38] may therefore exert their effect on LOV-domain photochemistry by a different mode of action than that of the Ile[16] variants characterized in this study. Further analysis of Asn[38] and Gln[43] will determine how mutation of these residues results in reduced photochemical reactivity.

ACKNOWLEDGMENT

We thank James Lewis and Istvan Szundi for assistance with data collection and analysis. We also thank Sharon Kelly and Stuart Sullivan for helpful comments on the manuscript and Brian Smith for generating Figure 8.

SUPPORTING INFORMATION AVAILABLE

Two figures as described in the text. This material is available free of charge via the Internet at http://pubs.acs.org.

REFERENCES

1. Briggs, W. R. (2006) Flavin-based photoreceptors in plants, in *Flavins—Photochemistry and Photobiology* (Silvia, E., and Edwards, A. M., Eds.) pp 183−216, RCS Publishing, Cambridge.
2. Batschauer, A. (2005) Plant cryptochromes: Their genes, biochemistry, and physiological roles, in *Handbook of Photosensory Receptors* (Briggs, W. R., and Spudich, J. L., Eds.) pp 2112−2146, Wiley-VCH, Weinheim.
3. Christie, J. M. (2007) Phototropin blue-light receptors, *Annu. Rev. Plant Biol.* (in press).
4. Huala, E., Oeller, P. W., Liscum, E., Han, I. S., Larsen, E., and Briggs, W. R. (1997) *Arabidopsis* NPH1: a protein kinase with a putative redox-sensing domain, *Science 278*, 2120−2123.
5. Christie, J. M., Reymond, P., Powell, G. K., Bernasconi, P., Raibekas, A. A., Liscum, E., and Briggs, W. R. (1998) Arabidopsis NPH1: a flavoprotein with the properties of a photoreceptor for phototropism, *Science 282*, 1698−1701.
6. Kagawa, T., Sakai, T., Suetsugu, N., Oikawa, K., Ishiguro, S., Kato, T., Tabata, S., Okada, K., and Wada, M. (2001) *Arabidopsis* NPL1: A phototropin homolog controlling the chloroplast high-light avoidance response, *Science 291*, 2138−2141.
7. Kinoshita, T., Doi, M., Suetsugu, N., Kagawa, T., Wada, M., and Shimazaki, K. (2001) Phot1 and phot2 mediate blue light regulation of stomatal opening, *Nature 414*, 656−660.
8. Takemiya, A., Inoue, S., Doi, M., Kinoshita, T., and Shimazaki, K. (2005) Phototropins promote plant growth in response to blue light in low light environments, *Plant Cell 17*, 1120−1127.
9. Sakamoto, K., and Briggs, W. R. (2002) Cellular and subcellular localization of phototropin 1, *Plant Cell 14*, 1723−1735.
10. Ohgishi, M., Saji, K., Okada, K., and Sakai, T. (2004) Functional analysis of each blue light receptor, cry1, cry2, phot1, and phot2, by using combinatorial multiple mutants in *Arabidopsis*, *Proc. Natl. Acad. Sci. U.S.A. 101*, 2223−2228.
11. Folta, K. M., and Spalding, E. P. (2001) Unexpected roles for cryptochrome 2 and phototropin revealed by high-resolution analysis of blue light-mediated hypocotyl growth inhibition, *Plant J. 26*, 471−478.
12. Taylor, B. L., and Zhulin, I. B. (1999) PAS domains: internal sensors of oxygen, redox potential, and light, *Microbiol. Mol. Biol. Rev. 63*, 479−506.
13. Salomon, M., Christie, J. M., Knieb, E., Lempert, U., and Briggs, W. R. (2000) Photochemical and mutational analysis of the FMN-binding domains of the plant blue light receptor, phototropin, *Biochemistry 39*, 9401−9410.
14. Kasahara, M., Swartz, T. E., Olney, M. A., Onodera, A., Mochizuki, N., Fukuzawa, H., Asamizu, E., Tabata, S., Kanegae, H., Takano, M., Christie, J. M., Nagatani, A., and Briggs, W. R. (2002) Photochemical properties of the flavin mononucleotide-binding domains of the phototropins from *Arabidopsis*, rice, and *Chlamydomonas reinhardtii*, *Plant Physiol. 129*, 762−773.
15. Christie, J. M., Swartz, T. E., Bogomolni, R. A., and Briggs, W. R. (2002) Phototropin LOV domains exhibit distinct roles in regulating photoreceptor function, *Plant J. 32*, 205−219.
16. Cho, H. Y., Tseng, T. S., Kaiserli, E., Sullivan, S., Christie, J. M., and Briggs, W. R. (2007) Physiological roles of the light,

oxygen, or voltage domains of phototropin 1 and phototropin 2 in *Arabidopsis*, *Plant Physiol. 143*, 517−529.
17. Jones, M. A., Feeney, K. A., Kelly, S. M., and Christie, J. M. (2007) Mutational analysis of phototropin 1 provides insights into the mechanism underlying LOV2 signal transmission, *J. Biol. Chem. 282*, 6405−6414.
18. Salomon, M., Lempert, U., and Rudiger, W. (2004) Dimerization of the plant photoreceptor phototropin is probably mediated by the LOV1 domain, *FEBS Lett. 572*, 8−10.
19. Nakasako, M., Iwata, T., Matsuoka, D., and Tokutomi, S. (2004) Light-induced structural changes of LOV domain-containing polypeptides from *Arabidopsis* phototropin 1 and 2 studied by small-angle X-ray scattering, *Biochemistry 43*, 14881−14890.
20. Matsuoka, D., and Tokutomi, S. (2005) Blue light-regulated molecular switch of Ser/Thr kinase in phototropin, *Proc. Natl. Acad. Sci. U.S.A. 102*, 13337−13342.
21. Kagawa, T., Kasahara, M., Abe, T., Yoshida, S., and Wada, M. (2004) Function analysis of phototropin2 using fern mutants deficient in blue light-induced chloroplast avoidance movement, *Plant Cell Physiol. 45*, 416−426.
22. Christie, J. M., Salomon, M., Nozue, K., Wada, M., and Briggs, W. R. (1999) LOV (light, oxygen, or voltage) domains of the blue-light photoreceptor phototropin (nph1): Binding sites for the chromophore flavin mononucleotide, *Proc. Natl. Acad. Sci. U.S.A. 96*, 8779−8783.
23. Swartz, T. E., Corchnoy, S. B., Christie, J. M., Lewis, J. W., Szundi, I., Briggs, W. R., and Bogomolni, R. A. (2001) The photocycle of a flavin-binding domain of the blue light photoreceptor phototropin, *J. Biol. Chem. 276*, 36493−36500.
24. Kennis, J. T. M., Crosson, S., Gauden, M., van Stokkum, I. H. M., Moffat, K., and van Grondelle, R. (2003) Primary reactions of the LOV2 domain of phototropin, a plant blue-light photoreceptor, *Biochemistry 42*, 3385−3392.
25. Kottke, T., Heberle, J., Hehn, D., Dick, B., and Hegemann, P. (2003) Phot-LOV1: Photocycle of a blue-light receptor domain from the green alga *Chlamydomonas reinhardtii*, *Biophys. J. 84*, 1192−1201.
26. Matsuoka, D., Iwata, T., Zikihara, K., Kandori, H., and Tokutomi, S. (2006) Primary processes during the light-signal transduction of phototropin, *Photochem. Photobiol.* (in press).
27. Swartz, T. E., Bogomolni, R. A., and Briggs, W. R. (2005) LOV-domain photochemistry, in *Handbook of Photosensory Receptors* (Briggs, W. R., and Spudich, J. L., Eds.) pp 305−322, Wiley-VCH, Weinheim.
28. Fedorov, R., Schlichting, I., Hartmann, E., Domratcheva, T., Fuhrmann, M., and Hegemann, P. (2003) Crystal structures and molecular mechanism of a light-induced signaling switch: The Phot-LOV1 domain from *Chlamydomonas reinhardtii*, *Biophys. J. 84*, 2474−2482.
29. Crosson, S., and Moffat, K. (2002) Photoexcited structure of a plant photoreceptor domain reveals a light-driven molecular switch, *Plant Cell 14*, 1067−1075.
30. Crosson, S., and Moffat, K. (2001) Structure of a flavin-binding plant photoreceptor domain: Insights into light-mediated signal transduction, *Proc. Natl. Acad. Sci. U.S.A. 98*, 2995−3000.
31. Lewis, J. W., and Kliger, D. S. (1993) *Rev. Sci. Instrum. 64*, 2828−2833.
32. Kliger, D. S., Lewis, J. W., and Randall, C. E. (1990) *Polarized Light in Optics and Spectroscopy*, Academic Press, Boston.
33. Corchnoy, S. B., Swartz, T. E., Lewis, J. W., Szundi, I., Briggs, W. R., and Bogomolni, R. A. (2003) Intramolecular proton transfers and structural changes during the photocycle of the LOV2 domain of phototropin 1, *J. Biol. Chem. 278*, 724−731.
34. Kelly, S. M., Jess, T. J., and Price, N. C. (2005) How to study proteins by circular dichroism, *Biochim. Biophys. Acta 1751*, 119−139.
35. Tsien, R. Y. (1998) The green fluorescent protein, *Annu. Rev. Biochem. 67*, 509−544.
36. Fischer, A. J., and Lagarias, J. C. (2004) Harnessing phytochrome's glowing potential, *Proc. Natl. Acad. Sci. U.S.A. 101*, 17334−17339.
37. Losi, A. (2006) Flavin-based photoreceptors in bacteria, in *Flavins−Photochemistry and Photobiology* (Silvia, E., and Edwards, A. M., Eds.) pp 217−269, RCS Publishing, Cambridge.
38. Briggs, W. R. (2007) The LOV domain: a chromophore module servicing multiple photoreceptors, *J. Biomed. Sci*. (in press).
39. Harper, S. M., Neil, L. C., and Gardner, K. H. (2003) Structural basis of a phototropin light switch, *Science 301*, 1541−1544.
40. Harper, S. M., Christie, J. M., and Gardner, K. H. (2004) Disruption of the LOV-J α helix interaction activates phototropin kinase activity, *Biochemistry 43*, 16184−16192.
41. Chen, E., Swartz, T. E., Bogomolni, R. A., and Kliger, D. S. (2007) A LOV story: The signaling state of the Phot1 LOV2 photocycle involves chromophore triggered protein structure relaxation, as probed by far-UV time-resolved optical rotatory spectroscopy, *Biochemistry* (in press).
42. Eitoku, T., Nakasone, Y., Matsuoka, D., Tokutomi, S., and Terazima, M. (2005) Conformational dynamics of phototropin 2 LOV2 domain with the linker upon photoexcitation, *J. Am. Chem. Soc. 127*, 13238−13244.
43. Harper, S. M., Neil, L. C., Day, I. J., Hore, P. J., and Gardner, K. H. (2004) Conformational changes in a photosensory LOV domain monitored by time-resolved NMR spectroscopy, *J. Am. Chem. Soc. 126*, 3390−3391.
44. Crosson, S., Rajagopal, S., and Moffat, K. (2003) The LOV domain family: Photoresponsive signaling modules coupled to diverse output domains, *Biochemistry 42*, 2−10.
45. Kottke, T., Hegemann, P., Dick, B., and Heberle, J. (2006) The photochemistry of the light-, oxygen-, and voltage-sensitive domains in the algal blue light receptor phot, *Biopolymers 82*, 373−378.
46. Alexandre, M. T. A., Arents, J. C., van Grondelle, R., Hellingwerf, K. J., and Kennis, J. T. M. (2007) A base-catalyzed mechanism for dark state recovery in the Avena sativa phototropin-1 LOV2 domain, *Biochemistry* (in press).

BI700852W